Heliyon 10 (2024) e26151

Contents lists available at ScienceDirect

Heliyon

journal homepage: www.cell.com/heliyon

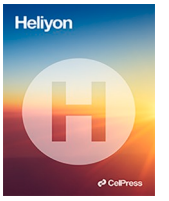

Research article

Numerical investigation on the wear characteristics of hip implant under static loading

Jaber E. Abu Qudeiri [a,*], Asarudheen Abdudeen [a,**], Mini Rema Sahadevan [b], Anantha Padmanabhan M [b]

[a] Mechanical and Aerospace Engineering Department, College of Engineering, United Arab Emirates University, Al Ain, 15551, United Arab Emirates
[b] Mechanical Engineering Department, College of Engineering Trivandrum, Thiruvananthapuram, India

ARTICLE INFO

Keywords:
Artificial hip implant
Contact pressure
Wear analysis
Design modification
Surface modification

ABSTRACT

Modern hip arthroplasty still faces the issue of wear in the articulating surface and wear induced debris. Thus, the design of hip implant is highly important for its longevity. Experimental demonstration of wear in hip implant involves both time and cost and, in this regard, finite element analysis acts as a suitable alternative. In this work, the wear characteristics of design modified and surface modified femoral head is studied. Femoral head is assumed to be made of Ti_6Al_4V and liner material is taken as UHMWPE. Design of the femoral head is modified by providing grooves on the femoral head as well as by providing an additional liner on the femoral head surface. Surface of the femoral head is modified with square or circular dimples. This work involves the development of femoral head model and its simulation using ANSYS under static load condition to get the contact pressure and sliding distance. Modified Archard's wear equation uses the contact stress and sliding distance to determine the wear volume produced per year and the obtained results are compared with that in the available literature. The study shows that the wear rate reduced up to 10% by surface modification and 3% by design modifications.

1. Introduction

The hip joint is a ball-and-socket synovial joint in the pelvis that connects the acetabulum and femur, which can transmit both static & dynamic loads with ease. It can transfer large dynamic loads (7–8 times the body weight) and can handle a wide variety of motions [1]. The hip joint is one of the essential joints which enables people to stand, walk, run, leap, sit, climbing stairs and bend [2]. Hip replacement surgery, also known as total hip arthroplasty (THA), involves replacing a damaged or injured hip joint with an artificial joint or implant [3,4]. Hip replacements are often done when arthritis cause significant hip pain and inflammation. Hip replacement surgery is also performed for a variety of causes, including hip fractures and natural wear and tear [3]. The method of surgery, design of implant, stem arrangement, the stability of fixation, weight of the patient and roughness of implant are some of the factors influencing the long-term survival of the prosthetic hip joint [5].

An artificial hip joint or hip implant can replace a damaged hip joint in two ways, either by total hip replacement (THR) or by partial hip replacement or hip resurfacing as shown in Fig. 1. In total hip replacement, implant which consists of stem, femoral head,

* Corresponding author.
** Corresponding author.
E-mail addresses: jqudeiri@uaeu.ac.ae (J.E. Abu Qudeiri), 201990133@uaeu.ac.ae (A. Abdudeen).

https://doi.org/10.1016/j.heliyon.2024.e26151
Received 6 July 2023; Received in revised form 7 February 2024; Accepted 8 February 2024
Available online 14 February 2024

acetabular cup and liner, is inserted into the medullary canal of femur bone with or without cement material and acetabular cup fits into the acetabulum [6]. In hip resurfacing, only the acetabular cup and femoral head are involved. An implant placed in touch with a bone, fuses with it gradually and this process is known as osseointegration.

Different types of biomaterials are used in hip implants, which includes metals, polymers, ceramics etc. [8]. Metal-on-Polyethylene (MoP), Metal-on-Metal (MoM), Ceramic-on-Ceramic (CoC), Ceramic-on-Polyethylene (COPE) are the common material combinations used in femoral head. Structural and microstructural studies of titanium alloys used in orthopedic implants are performed to guarantee its safe and successful usage [9]. The magnitude of load and the way in which it is carried out have an impact on the stresses developed in hip joints [10,11]. The release of metal ions from titanium implants, into the cells near the bone even in tiny levels can cause discomfort to the tissues around the implants [12]. Hip joint wear and the resulting temperature developed in the surrounding zone are numerically determined using finite element method [13]. von Mises stress and displacement in circular, elliptical, oval and trapezoidal stems are determined using finite element method by Anthony et al. [14]. Deformation and von Mises stresses are observed to be minimum for hip implant with trapezoidal stem of Cobalt chromium and acetabular cup of CoC [15]. Reduction in von Mises stresses was observed when femoral head size is increased and neck length is reduced [16]. Optimized cross section of trapezoidal shaped hip implant was determined using Design of Experiment (DoE) through ANSYSR-19 by Zuber et al. [17]. The wear and fatigue characteristics at the head-stem interface of hip implant made with Co–Cr–Mo-Alumina, Ti_6Al_4V-Alumina, and CoCrMo– Ti_6Al_4V combinations were numerically analysed by Manish et al. [18]. The fatigue behaviour was investigated with the help of Goodman's mean stress fatigue theory, whereas modified Archard's wear model was adopted to examine the wear rate.

Common biomaterials used for implant production include zirconia, zirconia-toughened alumina (ZTA), titanium alloys, stainless steel, special high-strength alloys, alumina, ultra-high molecular weight polyethylene (UHMWPE), and polytetrafluoroethylene (PTFE) [12,19–22]. For total hip arthroplasty (THA), commonly used metals and alloys include titanium alloys (Ti_6Al_4V), stainless steel, and cobalt-chromium-molybdenum alloys. These materials exhibit high corrosion resistance, wear resistance, toughness, and hardness compared to other metals and polymers [23]. Polymer materials, such as polytetrafluoroethylene (PTFE) and polyetheretherketone (PEEK), are favoured for low-friction hip replacements due to their excellent mechanical properties and wear resistance [24].

Note that, hip prosthesis is of two types: unipolar and bipolar. A stem, a femoral head, a liner, and an outer cup are comprised in the unipolar model, while a bipolar model constitutes a stem, a femoral head, an inner liner, an outer liner and an outer cup. Plastic material is placed as liner in between femoral head and outer cup since attaching plastic to metal is advantageous as it reduces tensile stresses at the edge of the contact zone and octahedral and maximum shear stresses directly beneath the load [25]. It also reduces friction and the following wear. Textured surfaces are frequently used on a wide range of mechanical components. Total hip arthroplasty with implants containing textured surface can minimize surface contact area, adhesion wear, and coefficient of friction [26]. Several studies have also demonstrated that surface texturing on contact surfaces improved tribological performance [27–30].

The existing hip implant model with femoral head, stem, liner, and backing material still faces issues with respect to osseointegration. Moreover, unstable fracture development, fatigue failures and inflammation in the presence of wear debris are reported while using the available designs and material combinations [5,31].

This study considered three modifications in the femoral head of the implant to reduce its wear. Two design modifications and a surface modification are proposed to reduce the area of contact and resulting contact stress. Continuous hemispherical grooves of varying width are a design modification which is aimed to reduce wear as well as to collect the wear debris. The second design modification is the provision of an additional liner of ultra-high molecular weight polyethylene (UHMWPE) in between femoral head and liner to prevent direct contact of metallic surface and plastic material [32]. As the surface modification dimples are placed randomly on the femoral head. A comparative analysis of circular and square shaped dimples is also done. All the analysis are done using finite element method software ANSYS. The contact pressure and sliding distance obtained from FEM analysis are used in the Archard's wear equation to determine the wear volume.

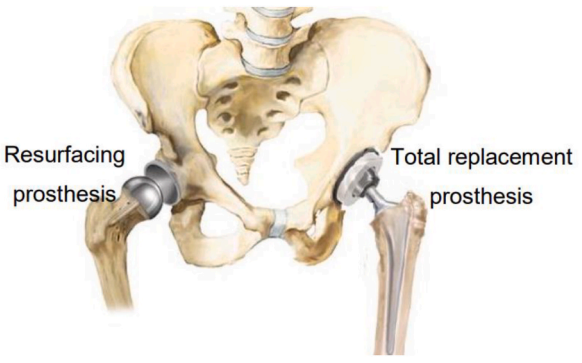

Fig. 1. Hip resurfacing and total hip replacement [7].

2. Numerical methodology

This section deals with the numerical model, governing equations, boundary conditions and validation of the numerical model.

The numerical model of the femoral head region consists of femoral head of diameter 32 mm made with Ti_6Al_4V, UHMWPE liner of 7 mm thick and an outer acetabular cup made with same titanium alloy as shown in Fig. 2 (a) and Fig. 2 (b). The model is considered without having any clearance between femoral head and liner. This model is finally simulated using Ansys workbench after applying all the boundary conditions.

2.1. Materials and geometric parameters used in the model

The materials used and geometric parameters chosen in this study are based on the data collected from literature. The material used for the femoral head is Ti_6Al_4V, liner material is ultra-high molecular weight polyethylene (UHMWPE) and outer acetabular cup material is Ti_6Al_4V. The dimensions used for the study are given in Table 1.

The material properties and material used for acetabular cup and liner are given in Table 2.

2.2. Boundary condition

In this study, finite element analysis of femoral head of an artificial hip joint implant is performed with various body weights under static loading condition. To ensure the safety of hip joint, Frank R et al. [33] has chosen the maximum weight applied to it in standing position as 6 to7 times the body weight. This research has considered up to an 850 N load which is almost equivalent to 85.0 Kg of human weight. The contact behaviour of hip joint parts is considered to be symmetric [34]. The contact algorithm used is the Augmented Lagrange technique. The load is applied on the top of acetabular cup surface in the z direction by keeping the spherical femoral head in fixed manner. The contact between the femoral head and liner is frictional and the liner is fixed with the acetabular cup as shown in Fig. 3.

Tetrahedral 10-node elements (Tet 10) were employed in ANSYS 20R1 for model meshing, with SOLID187 representing the femoral head assembly components. Contact surfaces were defined using CONTA174 and TARGE170. The chosen physics for meshing was mechanical, utilizing an adaptive size function.

2.3. Governing equations

The major parameters influencing the wear volume produced per year in a hip implant is contact pressure and sliding distance. The contact stress or contact pressure are discontinuous at all times and the contact region changes in a significant way and as result finite element methods are used to tackle such problems in a model to properly quantify the wear volume. Moreover, computational methods help to minimize the number of expensive experiments. The contact status of two bodies under static conditions is expressed in the matrix form is shown as equation (1).

$$[K]\{q\} = \{F\}^{ext} \tag{1}$$

where $\{F\}^{ext}$ is the external force, [K] is the combined stiffness matrix and {q} is the nodal displacement matrix [2]. The contact pressure between these articulating surfaces is calculated using the above equation and the obtained contact stress and sliding distance are applied directly into modified Archard's wear law for calculating wear volume, for a constant value of wear coefficient. The wear

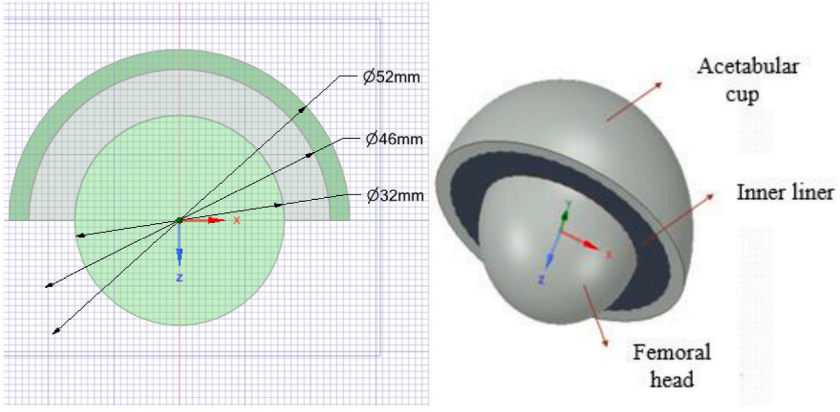

Fig. 2. a) cross sectional view of femoral head, liner and acetabular cup and b) 3D model of femoral head region.

Table 1
Dimensions of implant head.

Parts	Inner radius	Outer radius
Femoral head	0	16 mm
Liner	16 mm	23 mm
Outer cup	23 mm	26 mm

Table 2
Properties of bio materials chosen for the study.

Material	Density (g/cc)	Elastic modules (GPa)	Poisson's ratio
Ti6Al4V (Acetabular cup)	4.5	110	0.33
UHMWPE (Liner)	0.95	0.725	0.45

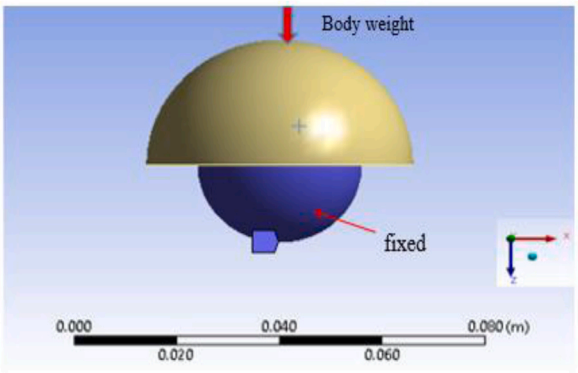

Fig. 3. Femoral head with boundary conditions and load applied.

volume is determined using modified Archard's wear law [1] shown in equation (2).

$$V = K_w \sigma_c A S_L \tag{2}$$

where, K_w is the wear coefficient in mm^3/Nm, $K_w = 0.235 \times 10^{-4} \times {R_a}^{2.03}$, V is the wear volume in mm^3, R_a is the surface roughness, S_L is the sliding distance in mm, σ_c is the contact pressure in MPa and A is the contact area in mm^2.

2.4. Validation

Validation is done on the femoral head model shown in Fig. 4, with dimensions taken from Vivek et al. [2], by keeping same boundary conditions and same loads. The material combination selected for the validation purpose is given in Table 3.

Different loads like 600 N, 650 N, 700 N, 750 N, 800 N and 850 N are applied on the top of the acetabular cup and contact pressure and sliding distance corresponding to each loading condition are extracted. The obtained values are used to determine the wear

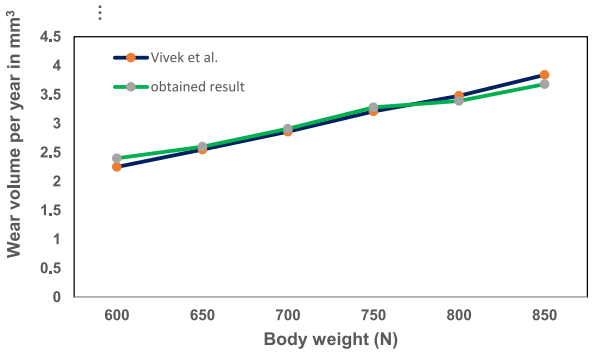

Fig. 4. Wear volume per year in mm^3 for Ti_6Al_4V - UHMWPE- Ti_6Al_4V combination under different body weights.

Table 3
Biomaterial combination used for validation of the numerical model.

Cases	Femoral head	Inner liner	Outer cup
Case 1	Ti_6Al_4V	UHMWPE	Ti_6Al_4V

volume produced per year from Archard's wear law. Wear volume per year in mm^3 for different body weights are plotted and compared with the results available in literature [2] is shown in Fig. 4.

3. Numerical analysis

The femoral head surface needs to be studied in different ways to solve the existing issues associated with the hip implant. Since wear is one of the major factors that reduces the longevity of a hip implant, the area of contact between femoral head and the liner part of acetabular component requires special attention. In this context, numerical analysis of three different surface/design modifications are considered in this study. Initially, surface modification of femoral head is done by providing semi-circular grooves. In this study, semi-circular grooves of different widths like 1 mm, 2 mm, 3 mm and 4 mm are provided on the femoral head surface, as shown in Fig. 5 (a), to reduce the area of contact in such way that there is reduced chance of adhesive wear as the liner debris get trapped inside those grooves. Fig. 5 (b) displays the cross-sectional view showing femoral head with groove, liner and acetabular cup. Here, femoral head and acetabular cup are considered to be made with Ti_6Al_4V and the liner material is taken as UHMWPE. Different body weights such as 600 N, 650 N, 700 N, 750 N, 800 N and 850 N are applied at the top of acetabular cup and the contact stress and sliding distance are determined for each load.

Secondly the nature of contact between femoral head and liner is changed. Metal on plastic type of contact between femoral head and liner is converted to plastic-on-plastic type of contact by attaching an additional liner material (UHMWPE) on the hemispherical surface of femoral head (Ti_6Al_4V) as shown in Fig. 6 (a) and the Cross sectional view of femoral head provided with additional liner is shown in Fig. 6 (b). By this modification, direct contact of harder material on a softer material can be prevented. Here the additional liner is fixed on the femoral head. The thickness of additional liner considered for the analysis are 1 mm, 2 mm and 3 mm. In all those cases the overall diameter of femoral head is kept as same.

Finally, the effectiveness of textures of different shape and same surface area on the wear characteristics is analysed. Here, surface area is fixed constant as 3.14 mm^2. Schematic diagram of textured surfaces considered for the study is given in Fig. 7 (a) and Fig. 7 (b). The circular dimples are of 2 mm and for square dimples edge length is 1.57 mm. Here, also the material combination used is same as that in case 1, the femoral head is made with titanium alloy (Ti_6Al_4V) and the liner is made with UHMWPE.

4. Results and discussion

In this section the results obtained from numerical models of surface modified and design modified femoral head under static loading condition are discussed. The wear volume per year for all these models are also determined. The numerical simulation of these models is done to obtain the maximum value of contact pressure and sliding distance. The static loading condition is assumed to minimize complexity of problem. Initially, femoral heads with grooves of 1 mm, 2 mm, 3 mm, and 4 mm widths are numerically analysed. The distribution of contract stress and sliding distance obtained for the femoral head with 1 mm wide groove, when subjected to 600 N force, is shown in Fig. 8 (a) and Fig. 8 (b). Here, the maximum value of contact pressure and sliding distance occurs at the central region and the minimum value occurs at circumferential region.

The maximum values of contact stress and sliding distance obtained for the femoral head with 1 mm wide groove under different

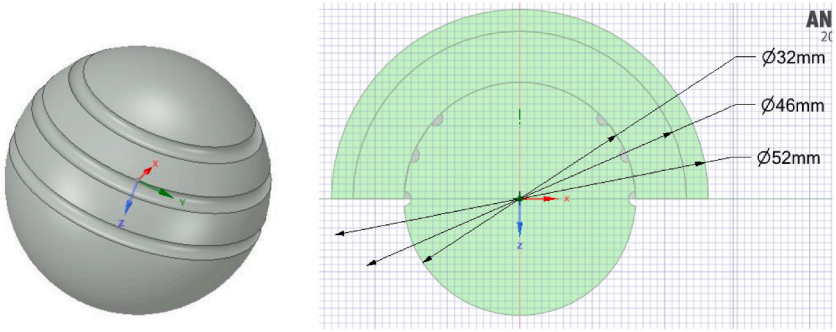

(a) (b)

Fig. 5. a) Femoral head model with semi-circular grooves and b) cross sectional view showing femoral head with groove, liner and acetabular cup.

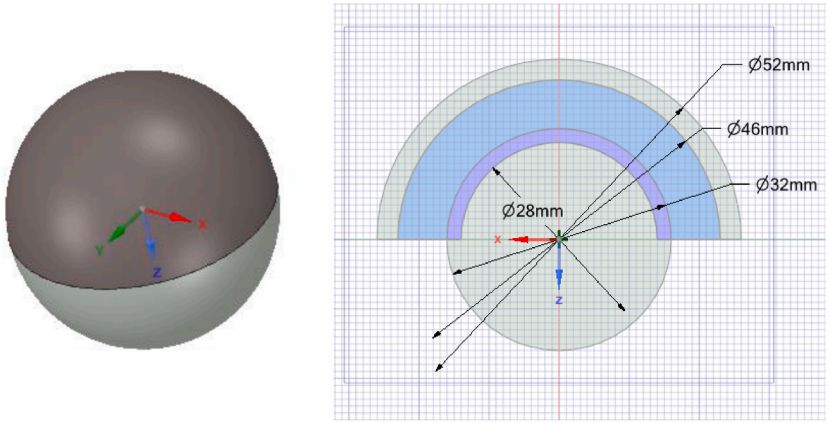

Fig. 6. a) Femoral head model with additional liner and b) Cross sectional view of femoral head provided with additional liner.

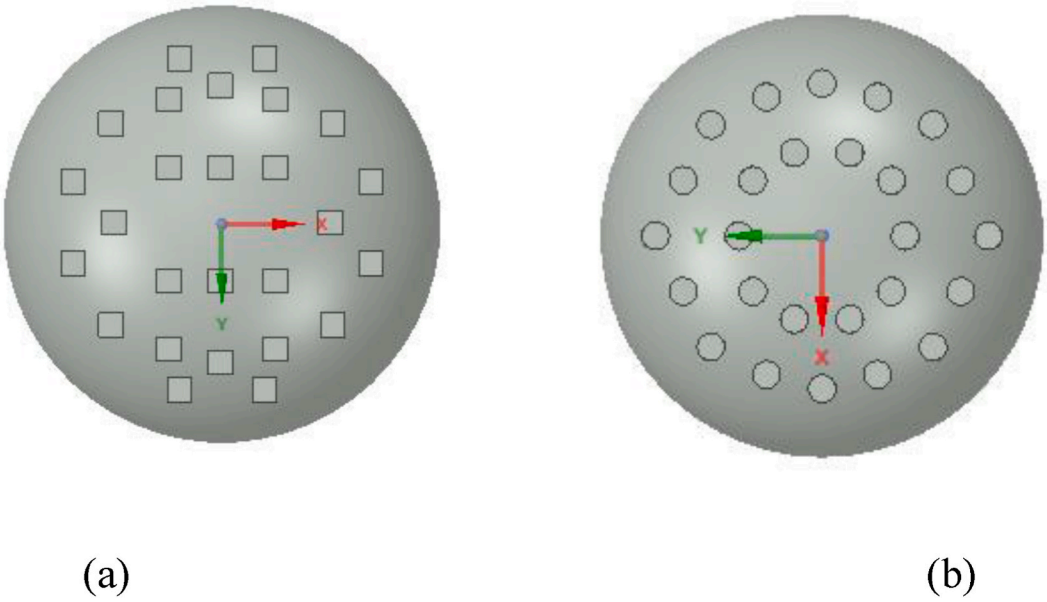

Fig. 7. Femoral head with a) square dimples of 1.57 mm edge length and b) Circular dimples of 2 mm diameter.

body weights is given in Fig. 9. Contact stress and sliding distance are increasing linearly with increase in body weight. In all the cases the maximum value is found at the central region of the femoral head.

Table 4 gives the maximum value of contact pressure and sliding distance obtained for femoral head with grooves of different widths under different body weights. In this study width of grooves are changed to see how it affects the contact pressure and sliding distance. It is observed that the wear volume reduced up to 10% when grooves of 1 mm width are provided on the femoral head.

Vivek et al. [2] observed better results when an additional liner was incorporated as a design modification. Here an additional liner of UHMWPE is placed between femoral head and liner to avoid the direct contact of metal on plastic. Additional liners with thickness 1 mm, 2 mm and 3 mm are considered for the analysis. The contact stress and sliding distance obtained for femoral head with additional liner of thickness 1 mm is shown in Fig. 10 (a) and Fig. 10 (b). Here also the maximum value of contact pressure and sliding distance occurs at the central region and the minimum value occurs at circumferential region.

To avoid redundancy in the presentation of results, authors have chosen to display the data for maximum contact pressure and sliding distance for only one variant in each surface modification in Fig. 11. However, it is important to note that the complete dataset, including values for all variants and surface modifications, is provided in the respective tables. Table 5 shows the complete data of contact pressure and sliding distance obtained for femoral head with additional liner of different thickness subjected to different loads. The contact pressure between femoral head surface and liner is less than that obtained to Vivek et al. [2], for the same boundary

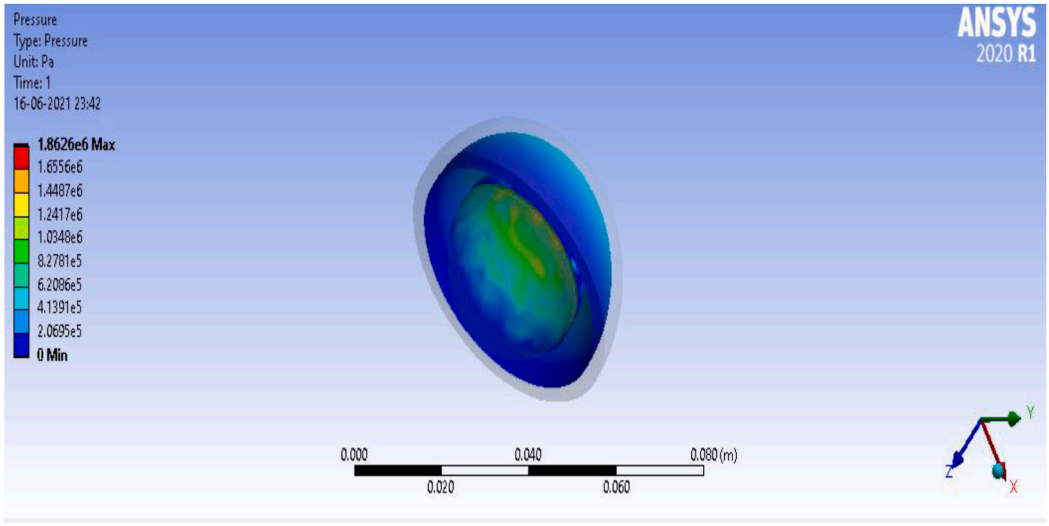

(a)

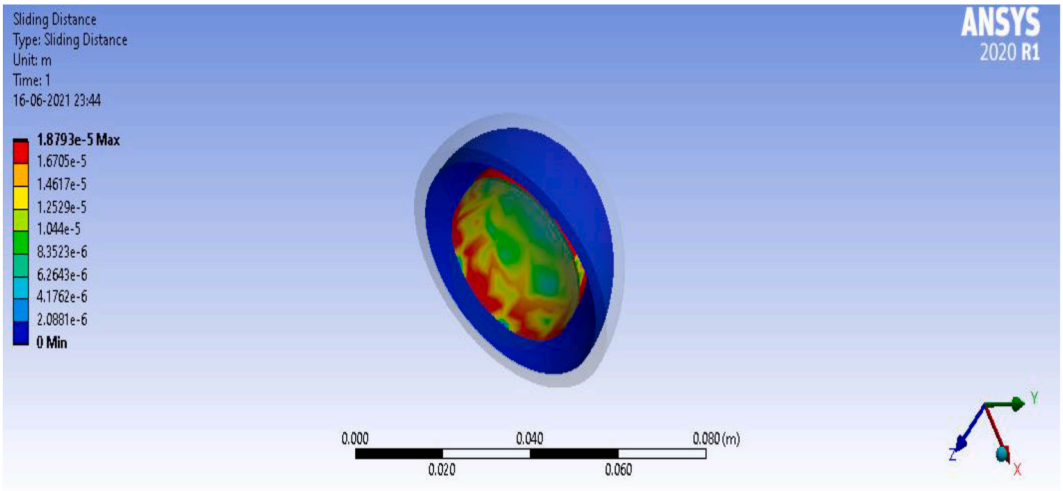

(b)

Fig. 8. a) Contact stress distribution b) sliding distance distribution.

conditions used.

When the thickness of additional liner increases, the contact pressure also increases but which is less than that obtained by Vivek et al. [2].

Finally circular and square dimples are made on the femoral head and a comparative analysis of contact stress and sliding distance is done. Table 6 shows the complete data of contact pressure and sliding distance obtained for femoral head with circular and square shaped dimples. It is observed that, the contact pressure and sliding distance obtained for square texture is higher than that of circular texture for all loads.

4.1. Wear volume

Wear volume is determined for both the surface modified and design modified femoral heads using modified Archard's wear law. Modified Archard's equation is mentioned in Equation (2). The contact pressure and sliding distance obtained from numerical analysis is used in the Archard's wear equation for the determination of wear volume. In the case of surface modification by providing semi-circular grooves, wear volume varies with groove size based on modified Archard's law. Even though the area of contact is reducing in each case, wear volume is increasing with increase in contact pressure and sliding distance.

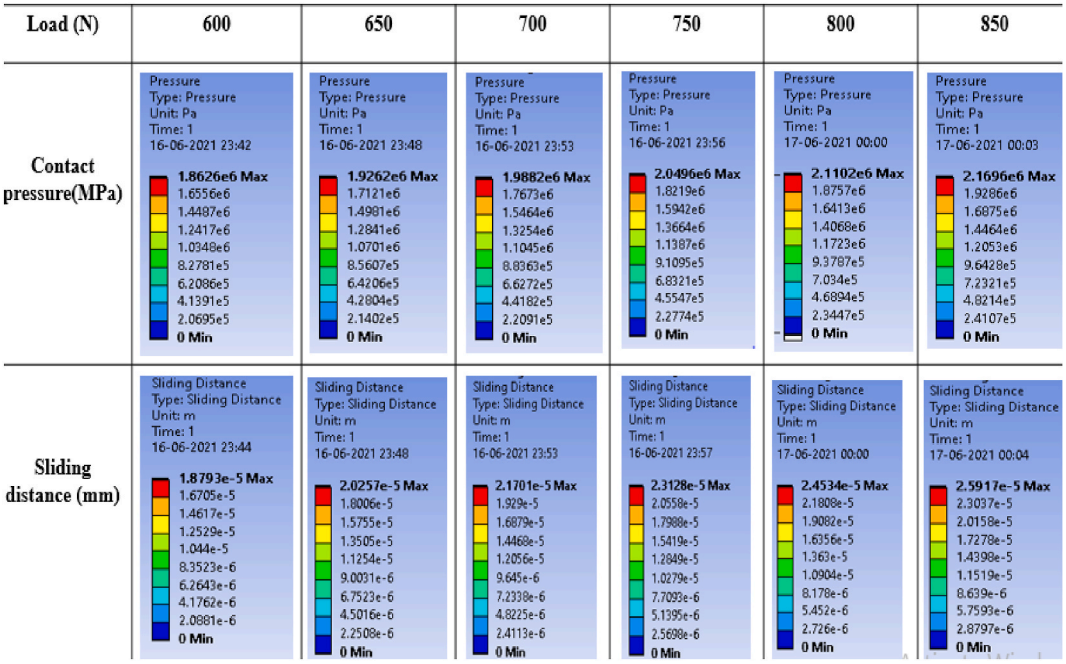

Fig. 9. The contact pressure and sliding distance for femoral head with 1 mm wide grooves on the surface under different body weights.

Table 4
Contact pressure and sliding distance for femoral head with grooves of different widths subjected to different loads.

Load (N)	Contact pressure (MPa)				Sliding distance (mm)			
	1 mm	2 mm	3 mm	4 mm	1 mm	2 mm	3 mm	4 mm
600	1.862	1.783	2.48	2.69	0.01879	0.0216	0.0209	0.021
650	1.926	1.868	2.59	2.81	0.0202	0.0232	0.0226	0.0226
700	1.988	1.951	2.7025	2.946	0.021	0.0247	0.0242	0.0241
750	2.049	2.0338	2.810	3.0725	0.0230	0.0263	0.0258	0.0257
800	2.06	2.122	2.919	3.197	0.0242	0.0278	0.0274	0.0272
850	2.16	2.2105	3.02	3.32	0.0259	0.0293	0.0289	0.0287

Wear volume (V) was calculated using modified Archard's wear equation (2), which provides a quantitative measure of the material loss due to wear in artificial hip implant components. The wear volume calculation is crucial for assessing the long-term performance and durability of these implants. To estimate the wear volume per year, further considerations were made. It was assumed that there are 10,000 cycles of loading per day, simulating typical daily activities. Additionally, the femoral surface roughness was assigned a value of 0.7 μm (micrometers), and the femoral radius was set at 16 mm. The contact area was determined by subtracting the cross-sectional area of surface modification from the hemispherical area, resulting in an area of 1608.5 mm^2.

The maximum contact stress and sliding distance data derived from rigorous numerical simulations were meticulously integrated into the wear volume equation. The ensuing product was subsequently scaled by a factor of 10,000 to accurately replicate daily loading cycles. Further scaling by a factor of 365 was executed to align the calculation with annual durations and an additional unit conversion factor of 1000 was applied to achieve results in mm3 per year. This meticulous and comprehensive computational approach not only yielded crucial insights into the wear characteristics of the hip implant components but also established a robust foundation for comparative analyses with extant literature. Collectively, these findings have significantly advanced in comprehension of the implants long-term performance and wear resistance, offering valuable contributions to the field. The calculation is shown in equation (3).

$$V = K_w \sigma_c A S_L * 10000 * 365 * 10^{-3} \left(mm^3 / year\right) \quad (3)$$

Fig. 12 depicts the variation in wear volume for femoral heads with grooves of different width subjected to different loads. The graph also compares the wear volume obtained by Vivek et al. [2] for the same material combination used. The results demonstrate that in the stand-up state for different body weight condition, femoral head with 4 mm wide groove succumbed the maximum wear. It is inferred that the wear volume of artificial hip joint implants decreases with increase in groove size. The higher wear volume observed in the 3 mm and 4 mm groove modifications is a result of the reduced contact area, which, in turn, leads to increased contact stress. This correlation is due to the inverse relationship between contact area and stress.

The modification of femoral head by the incorporation of an additional liner demonstrates that there is no considerable reduction of

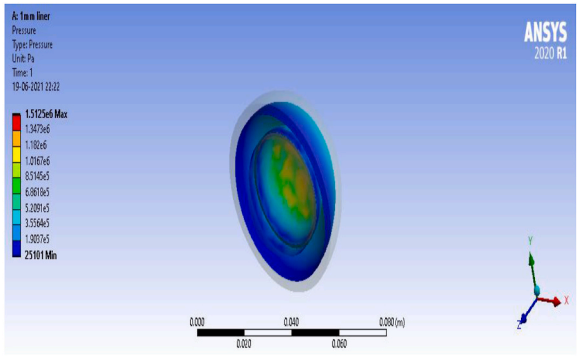

(a)

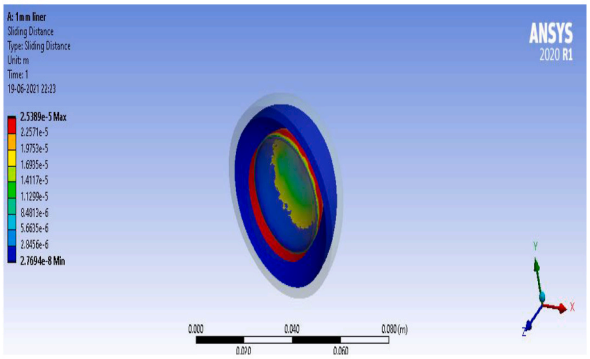

(b)

Fig. 10. a) Contact stress distribution and b) sliding distance distribution for femoral head with additional liner of 1 mm thickness.

Load (N)	600	650	700	750	800	850
Contact pressure(MPa)	A: 1mm liner Pressure Type: Pressure Unit: Pa Time: 1 19-06-2021 22:32 1.5125e6 Max 1.3473e6 1.182e6 1.0167e6 8.5145e5 6.8618e5 5.2091e5 3.5564e5 1.9037e5 25101 Min	A: 1mm liner Pressure Type: Pressure Unit: Pa Time: 1 19-06-2021 22:35 1.5932e6 Max 1.4193e6 1.2455e6 1.0716e6 8.9777e5 7.2392e5 5.5006e5 3.7621e5 2.0236e5 28510 Min	A: 1mm liner Pressure Type: Pressure Unit: Pa Time: 1 19-06-2021 22:37 1.6751e6 Max 1.4925e6 1.3099e6 1.1274e6 9.4479e5 7.6222e5 5.7965e5 3.9709e5 2.1452e5 31949 Min	A: 1mm liner Pressure Type: Pressure Unit: Pa Time: 1 19-06-2021 22:39 1.7568e6 Max 1.5655e6 1.3741e6 1.1828e6 9.9148e5 8.0015e5 6.0883e5 4.175e5 2.2617e5 34849 Min	A: 1mm liner Pressure Type: Pressure Unit: Pa Time: 1 19-06-2021 22:42 1.8397e6 Max 1.6393e6 1.4388e6 1.2384e6 1.038e6 8.3759e5 6.3718e5 4.3676e5 2.3635e5 35935 Min	A: 1mm liner Pressure Type: Pressure Unit: Pa Time: 1 19-06-2021 22:45 1.9229e6 Max 1.7134e6 1.5038e6 1.2943e6 1.0847e6 8.7513e5 6.6556e5 4.56e5 2.4644e5 36874 Min
Sliding distance (mm)	A: 1mm liner Sliding Distance Type: Sliding Distance Unit: m Time: 1 19-06-2021 22:34 2.5389e-5 Max 2.2571e-5 1.9753e-5 1.6935e-5 1.4117e-5 1.1299e-5 8.4813e-6 5.6635e-6 2.8456e-6 2.7694e-8 Min	A: 1mm liner Sliding Distance Type: Sliding Distance Unit: m Time: 1 19-06-2021 22:36 2.7407e-5 Max 2.4365e-5 2.1323e-5 1.8281e-5 1.5239e-5 1.2196e-5 9.1542e-6 6.112e-6 3.0699e-6 2.7672e-8 Min	A: 1mm liner Sliding Distance Type: Sliding Distance Unit: m Time: 1 19-06-2021 22:38 2.9413e-5 Max 2.6148e-5 2.2883e-5 1.9618e-5 1.6353e-5 1.3088e-5 9.8233e-6 6.5583e-6 3.2933e-6 2.8292e-8 Min	A: 1mm liner Sliding Distance Type: Sliding Distance Unit: m Time: 1 19-06-2021 22:40 3.1411e-5 Max 2.7924e-5 2.4438e-5 2.0951e-5 1.7464e-5 1.3977e-5 1.049e-5 7.0031e-6 3.5162e-6 2.9342e-8 Min	A: 1mm liner Sliding Distance Type: Sliding Distance Unit: m Time: 1 19-06-2021 22:43 3.3384e-5 Max 2.9678e-5 2.5972e-5 2.2266e-5 1.856e-5 1.4854e-5 1.1148e-5 7.4425e-6 3.7366e-6 3.067e-8 Min	A: 1mm liner Sliding Distance Type: Sliding Distance Unit: m Time: 1 19-06-2021 22:45 3.5331e-5 Max 3.1408e-5 2.7486e-5 2.3564e-5 1.9642e-5 1.572e-5 1.1798e-5 7.8761e-6 3.954e-6 3.1922e-8 Min

Fig. 11. Contact pressure and sliding distance obtained for the femoral head in the presence of additional liner of 1 mm thickness for all loads.

Table 5
Contact pressure and sliding distance for femoral head with additional liner.

Load (N)	Contact pressure (MPa)			Sliding distance (mm)		
	1 mm	2 mm	3 mm	1 mm	2 mm	3 mm
600	1.5125	1.6903	1.9310	0.0253	0.0209	0.0169
650	1.5932	1.7816	2.0316	0.0274	0.0226	0.0185
700	1.6751	1.8700	2.1305	0.0294	0.0243	0.0199
750	1.7568	1.9576	2.2276	0.0314	0.0259	0.0214
800	1.8397	2.0439	2.3236	0.033	0.0275	0.0229
850	1.9229	2.1297	2.4173	0.0353	0.0292	0.0243

Table 6
Contact pressure and sliding distance for femoral head with circular and square shaped dimples.

Load (N)	Circular hole		Square hole	
	Contact pressure (MPa)	Sliding distance (mm)	Contact pressure (MPa)	Sliding distance (mm)
600	3.3305	0.0106	4.335	0.01209
650	3.4289	0.0116	4.475	0.0133
700	3.5243	0.01258	4.483	0.01447
750	3.618	0.01352	4.687	0.01562
800	3.7107	0.01446	4.788	0.0167
850	3.8005	0.0154	4.887	0.0178

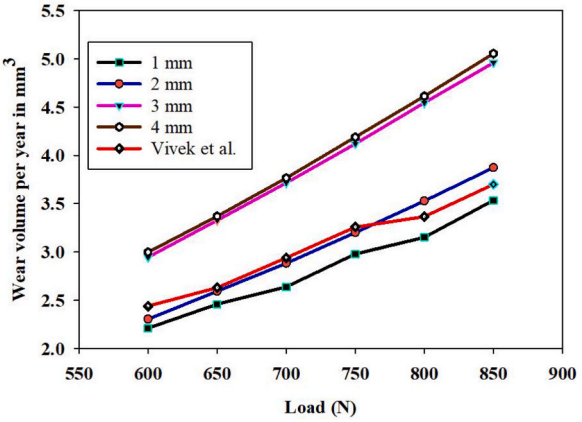

Fig. 12. Variation of wear volume with body weight for femoral head with grooves of 1 mm, 2 mm, 3 mm and 4 mm thickness.

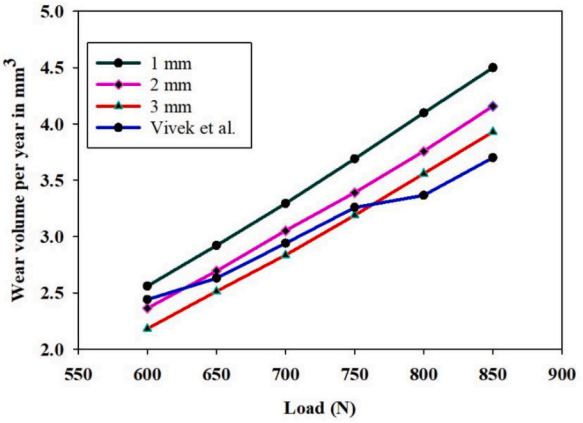

Fig. 13. Variation of wear volume with body weight in the presence of additional liner different thickness.

wear volume when an additional liner is attached on the femoral head surface. It is getting decreased when additional liner thickness is increasing. Fig. 13 depicts the variation in wear volume for femoral heads with additional liners of different thickness subjected to different loads. The graph also gives a comparison of the results of wear volume obtained by Vivek et al. [2] for the same material combination used. The results demonstrate that in the stand-up state for different body weight condition, the wear mostly occurs in 1 mm thick additional liner. When femoral head was attached with additional liner of 3 mm, the wear volume has the lowest value. It is inferred that the wear volume of femoral head region of implant is getting reduced when the thickness of additional liner is increased. The molecules situated on the upper surface of a thin liner exhibit less resistance to deformation in comparison to thicker liners. This disparity results in greater sliding distances and consequently leads to higher wear volume in thin liners as opposed to thicker ones.

The wear volume per year is minimum for circular dimples. It is also observed that wear volume, increases linearly with body weight as shown in Fig. 14.

5. Conclusion

This study employed finite element analysis to investigate the wear characteristics of a design-modified and surface-modified femoral head, with a primary focus on estimating the annual wear volume. By applying the well-established modified Archard's wear law, authors were able to estimate and compare the wear results with existing literature, providing valuable insights into the field of orthopaedic implant wear.

The findings emphasize that wear behaviour is not solely dictated by material properties but also influenced by the contact surface area between the femoral head and acetabular cup. Although the incorporation of an additional liner between the femoral head and liner did not yield significant reductions in wear volume, authors discovered a more promising solution through the implementation of grooves on the femoral head. These grooves effectively reduced wear volume while concurrently serving as debris traps, mitigating adhesive wear and potentially enhancing implant longevity.

Furthermore, a comparative analysis of femoral heads featuring circular and square dimples revealed that the adoption of circular dimples resulted in a noticeable decrease in wear volume compared to their square counterparts. This finding suggests the potential benefits of optimizing femoral head surface characteristics to achieve superior wear performance.

Overall, the modification of the femoral head design proved to be a crucial factor in reducing contact pressure, consequently lowering the risk of implant failure. The implications of this research extend beyond theoretical considerations, as it has practical relevance within the field of orthopaedic implant development.

By addressing the wear-related challenges associated with femoral head and acetabular cup interfaces, this study contributes valuable insights to the scientific community. Outcomes of the research can inform the design and development of orthopaedic implants with improved wear resistance, thereby enhancing patient outcomes and ensuring the long-term success of these crucial medical interventions.

6. Limitations and future scope

While this study provides valuable insights into the wear characteristics of hip implants under static loading, it is important to acknowledge certain limitations. The research primarily focuses on static loading conditions, and future investigations should expand into dynamic loading scenarios and potential wear issues related to the fixation of additional liner to better emulate real-world conditions.

Additionally, the study does not consider the potential effects of tribo corrosion or the long-term durability of hip implants, warranting further research in these areas. To enhance the field's applicability and impact, future research should also explore innovative biomaterials, surface coatings, and patient-specific implant designs to reduce wear and improve implant longevity. Collaborations with clinical researchers for validation, advanced wear testing methods, and comprehensive cost-effectiveness analyses should be prioritized. Addressing these limitations and embracing these future research directions will contribute to the development

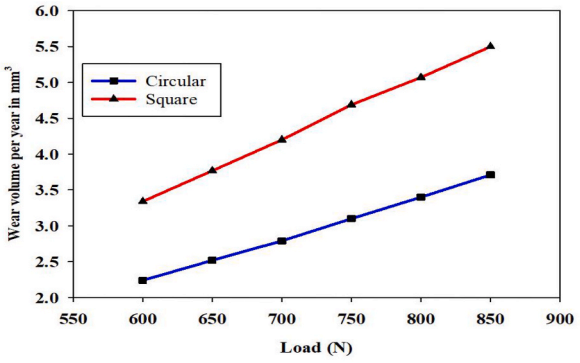

Fig. 14. Wear volume against body weight for femoral head with circular and square dimples.

of safer and more durable hip implants, ultimately benefiting patients and healthcare systems alike.

Funding

This research is supported by the Research Office of UAE University, UAE, grant numbers 12N020 and 31N424.

Data availability statement

The authors have not deposited the data associated with this study into a publicly available repository. The data used in this study is confidential and, as such, has not been made publicly accessible.

CRediT authorship contribution statement

Jaber E. Abu Qudeiri: Supervision, Project administration, Funding acquisition, Conceptualization. **Asarudheen Abdudeen:** Writing – review & editing, Writing – original draft, Visualization, Validation, Supervision, Software, Resources, Project administration, Methodology, Investigation, Formal analysis, Data curation, Conceptualization. **Mini Rema Sahadevan:** Writing – review & editing, Writing – original draft, Supervision, Project administration, Formal analysis, Data curation. **Anantha Padmanabhan M:** Writing – original draft, Validation, Software, Methodology, Investigation.

Declaration of competing interest

The authors declare the following financial interests/personal relationships which may be considered as potential competing interests: Jaber E. Abu Qudeiri, Asarudheen Abdudeen, Mini Rema Sahadevan, Anantha Padmanabhan M has patent #US 11, 672, 666 B1 issued to United Arab Emirates University, Alain.

References

[1] J.S.-S. Wu, J.-P. Hung, C.-S. Shu, J.-H. Chen, The computer simulation of wear behavior appearing in total hip prosthesis, Comput. Methods Progr. Biomed. 70 (2003) 81–91.
[2] V. Jangid, A.K. Singh, A. Mishra, Wear simulation of artificial hip joints: effect of materials, Mater. Today Proc. 18 (2019) 3867–3875.
[3] R. Case, Pearl River Library March 23 (1995) 1995.
[4] K.N. Chethan, B.S. Shenoy, N.S. Bhat, Role of different orthopedic biomaterials on wear of hip joint prosthesis: a review, Mater. Today Proc. 5 (2018) 20827–20836.
[5] A. Bashiri, H.E.M. Sallam, A.A. Abd-Elhady, Progressive failure analysis of a hip joint based on extended finite element method, Eng. Fail. Anal. 117 (2020) 104829.
[6] A. Abdudeen, J.E. Abu Qudeiri, A. Kareem, A.K. Valappil, Latest developments and insights of orthopedic implants in biomaterials using additive manufacturing technologies, J. Manufacturing and Materials Processing 6 (2022) 162.
[7] E. Askari, P. Flores, D. Dabirrahmani, R. Appleyard, A review of squeaking in ceramic total hip prostheses, Tribol. Int. 93 (2016) 239–256.
[8] M. Merola, S. Affatato, Materials for hip prostheses: a review of wear and loading considerations, Materials 12 (2019) 495.
[9] M. Kaur, K. Singh, Review on titanium and titanium based alloys as biomaterials for orthopaedic applications, Mater. Sci. Eng. C 102 (2019) 844–862.
[10] B. Levine, C.J. Della Valle, J.J. Jacobs, Applications of porous tantalum in total hip arthroplasty, J. Am. Acad. Orthop. Surg. (2006), https://doi.org/10.5435/00124635-200611000-00008.
[11] G. Bergmann, G. Deuretzbacher, M. Heller, F. Graichen, A. Rohlmann, J. Strauss, G.N. Duda, Hip contact forces and gait patterns from routine activities, J. Biomech. 34 (2001) 859–871.
[12] T.R. Rautray, R. Narayanan, K.-H. Kim, Ion implantation of titanium based biomaterials, Prog. Mater. Sci. 56 (2011) 1137–1177.
[13] J.C. Fialho, P.R. Fernandes, L. Eça, J. Folgado, Computational hip joint simulator for wear and heat generation, J. Biomech. 40 (2007) 2358–2366.
[14] C. Dopico Gonzalez, Probabilistic Finite Element Analysis of the Uncemented Total Hip Replacement, 2009.
[15] K.N. Chethan, M. Zuber, S. Shenoy, C.R. Kini, Static structural analysis of different stem designs used in total hip arthroplasty using finite element method, Heliyon 5 (2019) e01767.
[16] K.N. Chethan, N.S. Bhat, M. Zuber, B.S. Shenoy, Finite element analysis of hip implant with varying in taper neck lengths under static loading conditions, Comput. Methods Progr. Biomed. 208 (2021) 106273.
[17] C. Kn, M. Zuber, S. Bhat N, S. Shenoy B, Optimized trapezoidal-shaped hip implant for total hip arthroplasty using finite element analysis, Cogent Eng 7 (2020) 1719575.
[18] M. Belwanshi, P. Jayaswal, A. Aherwar, Wear and fatigue behaviour investigation of hip implant head-stem interface using finite element analysis, Mater. Today Proc. 56 (2021) 2893–2901.
[19] S. Ghosh, S. Sanghavi, P. Sancheti, Metallic biomaterial for bone support and replacement, in: Fundamental Biomaterials: Metals, Elsevier, 2018, pp. 139–165.
[20] A. Civantos, E. Martínez-Campos, V. Ramos, C. Elvira, A. Gallardo, A. Abarrategi, Titanium coatings and surface modifications: toward clinically useful bioactive implants, ACS Biomater. Sci. Eng. 3 (2017) 1245–1261.
[21] K. Moghadasi, M.S.M. Isa, M.A. Ariffin, S. Raja, B. Wu, M. Yamani, M.R. Bin Muhamad, F. Yusof, M.F. Jamaludin, M.S. bin Ab Karim, A review on biomedical implant materials and the effect of friction stir based techniques on their mechanical and tribological properties, J. Mater. Res. Technol. 17 (2022) 1054–1121.
[22] L. Guo, S.A. Naghavi, Z. Wang, S.N. Varma, Z. Han, Z. Yao, L. Wang, L. Wang, C. Liu, On the design evolution of hip implants: a review, Mater. Des. 216 (2022) 110552.
[23] M. Zhou, H. Sun, Y. Gan, C. Ji, Y. Chen, Y. Lu, J. Lin, Q. Wang, Tuning the Corrosion Resistance, Antibacterial Activity, and Cytocompatibility by Constructing Grooves on the Surface of Ti6al4v3cu Alloy, Antibacterial Activity, and Cytocompatibility by Constructing Grooves on the Surface of Ti6al4v3cu Alloy (n.d.).
[24] L. Savin, T. Pinteala, D.N. Mihai, D. Mihailescu, S.S. Miu, M.T. Sirbu, B. Veliceasa, D.C. Popescu, P.D. Sirbu, N. Forna, Updates on biomaterials used in total hip arthroplasty (THA), Polymers 15 (2023) 3278.
[25] D.L. Bartel, A.H. Burstein, M.D. Toda, D.L. Edwards, The Effect of Conformity and Plastic Thickness on Contact Stresses in Metal-Backed Plastic Implants, 1985.
[26] J. Jamari, M.I. Ammarullah, A.P.M. Saad, A. Syahrom, M. Uddin, E. van der Heide, H. Basri, The effect of bottom profile dimples on the femoral head on wear in metal-on-metal total hip arthroplasty, J. Funct. Biomater. 12 (2021) 38.
[27] M.I. Ammarullah, A.P.M. Saad, A. Syahrom, H. Basri, Contact pressure analysis of acetabular cup surface with dimple addition on total hip arthroplasty using finite element method, in: IOP Conf Ser Mater Sci Eng, IOP Publishing, 2021 12001.

[28] W. Wang, Y. He, Y. Li, B. Wei, Y. Hu, J. Luo, Investigation on Inner Flow Field Characteristics of Groove Textures in Fully Lubricated Thrust Bearings, Industrial Lubrication and Tribology, 2018.
[29] T. Pratap, K. Patra, Mechanical micro-texturing of Ti-6Al-4V surfaces for improved wettability and bio-tribological performances, Surf. Coat. Technol. 349 (2018) 71–81.
[30] D. Choudhury, M. Vrbka, A. Bin Mamat, I. Stavness, C.K. Roy, R. Mootanah, I. Krupka, The impact of surface and geometry on coefficient of friction of artificial hip joints, J. Mech. Behav. Biomed. Mater. 72 (2017) 192–199.
[31] A. Sedmak, K. Čolić, A. Grbović, I. Balać, M. Burzić, Numerical analysis of fatigue crack growth of hip implant, Eng. Fract. Mech. 216 (2019) 106492.
[32] J. Abu Qudeiri, A. Abdudeen, M.R. Sahadevan, Hip Implant with Reduced Wear, 2023.
[33] R.M. Frank, M.A. Slabaugh, R.C. Grumet, W.W. Virkus, C.A. Bush-Joseph, S.J. Nho, Posterior hip pain in an athletic population: differential diagnosis and treatment options, Sport Health 2 (2010) 237–246.
[34] A. Vulović, N. Filipovic, Computational Analysis of Hip Implant Surfaces, 2019.